Decay of the Dst field of geomagnetic disturbance after substorm onset and its implication to storm-substorm relation

T. Iyemori[1], D. R. K. Rao[2]

[1] Faculty of Science, Kyoto University, Kyoto 606-01, Japan
[2] Indian Institute of Geomagnetism, Bombay 400 005, India

Abstract. In order to investigate the causal relationship between magnetic storms and substorms, variations of the mid-latitude geomagnetic indices, ASY (asymmetric part) and SYM (symmetric part), at substorm onsets are examined. Substorm onsets are defined by three different phenomena; (1) a rapid increase in the mid-latitude asymmetric-disturbance indices, ASY-D and ASY-H, with a shape of so-called 'mid-latitude positive bay'; (2) a sharp decrease in the AL index; (3) an onset of Pi2 geomagnetic pulsation. The positive bays are selected using eye inspection and a pattern-matching technique. The 1-min-resolution SYM-H index, which is essentially the same as the hourly Dst index except in terms of the time resolution, does not show any statistically significant development after the onset of substorms; it tends to decay after the onset rather than to develop. It is suggested by a simple model calculation that the decay of the magnetospheric tail current after substorm onset is responsible for the decay of the Dst field. The relation between the IMF southward turning and the development of the Dst field is reexamined. The results support the idea that the geomagnetic storms and substorms are independent processes; that is, the ring-current development is not the result of the frequent occurrence of substorms, but that of enhanced convection caused by the large southward IMF. A substorm is the process of energy dissipation in the magnetosphere, and its contribution to the storm-time ring-current formation seems to be negligible. The decay of the Dst field after a substorm onset is explained by a magnetospheric energy theorem.

1 Introduction

A geomagnetic storm is usually defined as a large decrease in the horizontal component of geomagnetic field in middle or low latitudes ($\delta H \leq -50$ nT), the decrease being mainly caused by a development of the equatorial ring current. A substorm is usually defined as a sequence of the process in the polar region which is characterized by a sudden auroral brightening and subsequent intensification of auroral electrojets (e.g. Akasofu and Chapman, 1972; Rostoker et al., 1980, and references therein). A substorm onset is often identified by a sudden increase in the AE indices, by an onset of Pi2 micropulsations, or by commencement of mid-latitude positive bay (Rostoker et al., 1980). Geomagnetic storms and substorms are closely related, in the sense that both are developed when the interplanetary magnetic field (IMF) has a strong southward component. However, there are two (or more) different scenarios on the causal relationship among southward IMF, substorms, and storms. One idea (scenario A) is that the southward IMF drives substorms, and the particles injected into the inner magnetosphere in the substorm process form the ring-current; that is, the frequent occurrence of substorms is the cause of a geomagnetic storm defined by the ring-current development. Another idea (scenario B) is that both the substorms and the storms are caused by the enhanced magnetospheric convection under southward IMF conditions; that is, the particle injection associated with the enhanced convection (enhanced dawn-to-dusk electric field) is the cause of the storm-time ring-current formation, and the substorms are the independent processes having the same origin. This means that the inflow of the solar-wind energy is controlled by the southward component of the IMF (Kamide, 1992; Gonzalez et al., 1994, and references therein).

After a substorm onset, energetic-particle injection is observed at synchronous orbit and the hourly Dst index becomes significant in magnitude (e.g. Kamide and McIlwain, 1974). So far, no storm, i.e. no large Dst-index development, has been reported without any substorm activity defined by sudden auroral-electrojet intensification indicated by the AE indices. These facts provide evidence for scenario A.

On the other hand, Russell et al. (1974) showed that the southward IMF is the controlling factor of Dst

Correspondence to: T. Iyemori

development, rather than the AE index. Clauer and McPherron (1980) and Clauer et al. (1983) also showed that the response of the asymmetric disturbance of the mid-latitude geomagnetic field has better correlation with the IMF southward component than with the AL index which is a measure of the westward auroral-electrojet intensity.

The mid-latitude geomagnetic disturbance is not symmetric in longitude, but generally has strong asymmetry. Such asymmetric nature has been attributed to the so-called 'partial ring current' (e.g. Fukushima and Kamide, 1973) and to the various current systems that have been proposed to explain the geomagnetic disturbances on the ground. If the asymmetric disturbance is caused by the asymmetric development of the ring current, the better correlation of this disturbance with the IMF suggests direct causal relation between the IMF and the ring-current development without the substorm process between them. This fact supports scenario B. Kamide (1992) reviewed and discussed the relation between substorms and storms, and presented a working model.

In this paper, we try to investigate the relation between the ring-current development and substorm onset using the 1-min-resolution SYM-H, ASY-D and ASY-H indices (Iyemori, 1990; Iyemori et al., 1992). The SYM-H is essentially a high-time-resolution Dst index, and hence a measure of the ring-current energy (Dessler and Parker, 1959; Scopke, 1966) including its magnetic energy (e.g. Siscoe, 1970). The ASY-H index is essentially the same as that used by Clauer and McPherron (1980) and Clauer et al. (1983), and the ASY-D index is the D- (declination-) component version similar to the ASY-H index introduced by Iyemori (1990). Various current systems in the magnetosphere, such as the asymmetric ring current, the field-aligned currents or the substorm wedge current, contribute to the asymmetric magnetic disturbance on the ground. The ASY indices indicate the effects of these current systems. A mid-latitude positive bay seen in the ASY-D and -H indices is used in this paper to determine the onset time of a substorm. We also use a sharp decrease in the AL index or a clear onset of Pi2 geomagnetic pulsation to define a substorm onset and examine the variation of the Dst field after the substorm onsets for these three different criteria of event selection.

2 Mid-latitude ASY and SYM indices

To describe geomagnetic disturbance fields in the mid-latitudes with high-time-resolution (i.e. 1 min), ASY- and SYM-disturbance indices are introduced and derived for both H and D components; that is, for the components in the horizontal (dipole) direction H (SYM-H, ASY-H) and in the orthogonal (east-west) direction D (SYM-D, ASY-D) (Iyemori, 1990; Iyemori et al., 1992). The symmetric disturbance field in H, SYM-H, is essentially the same as Sugiura's hourly Dst index (Sugiura and Poros, 1971), although 1-min values from different sets of stations and a slightly different coordinate system are used. Similarly, ASY-H is close to the asymmetric indices proposed by Kawasaki and Akasofu (1971), Crooker and Siscoe (1971), and Clauer et al. (1983). The ASY-D used in this paper was introduced and discussed by Iyemori (1990), and the method of derivation is essentially the same as that of ASY-H.
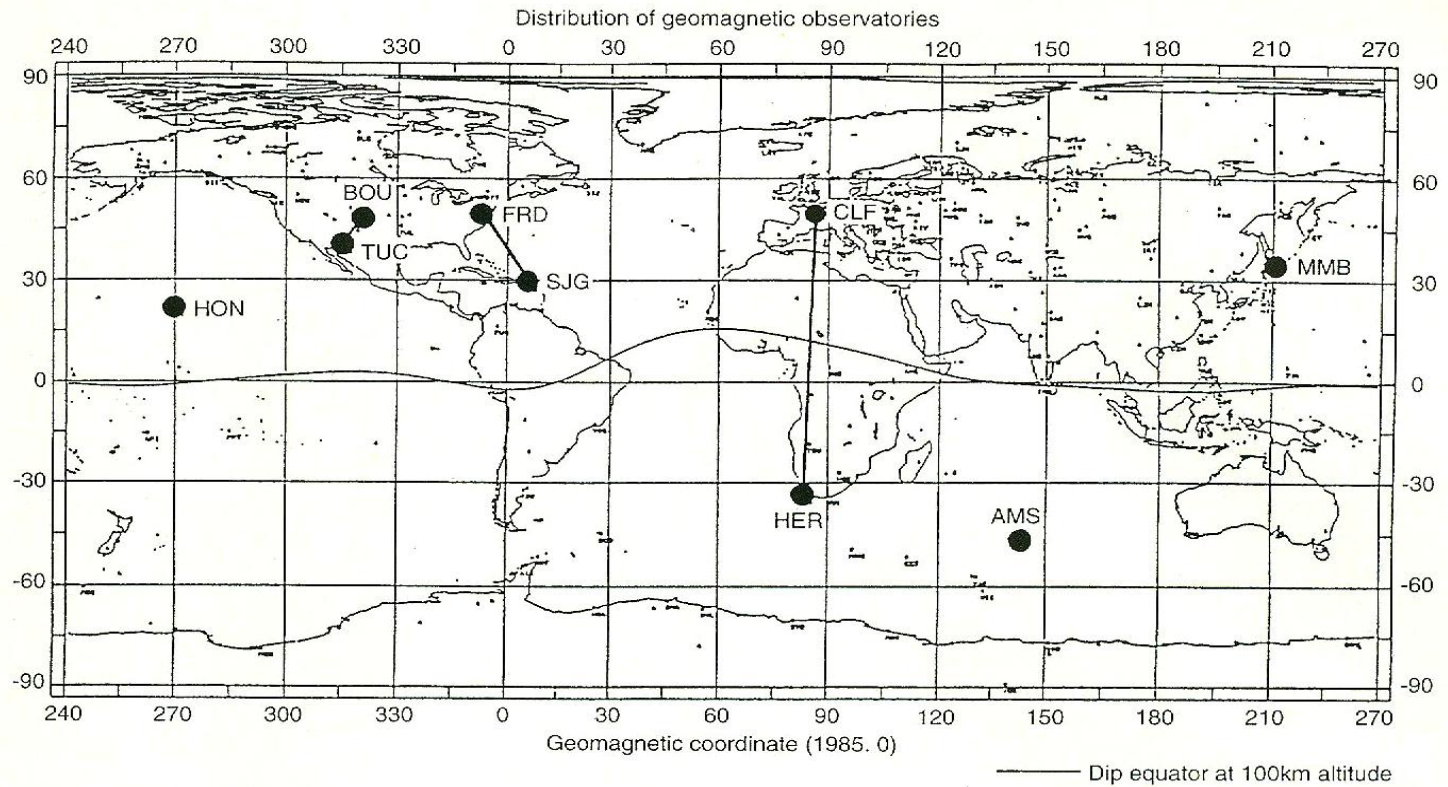
Given in Table 1, and also shown in Fig. 1, are the geomagnetic observatories used for scaling the indices along with their respective geomagnetic dipole coordinates. It may be noted that some of the stations used for deriving the ASY and SYM indices, viz. Fredericksburg, Boulder, Tucson, Memambetsu, Martin de Vivies and Chambon-la-Foret, are at higher latitudes than those used in the derivation of Sugiura's standard Dst index (Honolulu, Kakioka, Hermanus and San Juan). Only six of the stations among those in Table 1 are used for the derivation of indices at each of the months, some stations being replaced by others depending on the availability and the quality of the data in that month. The derivation procedure essentially consists of the following four steps:

- Subtraction of the geomagnetic main field and the Sq (solar quiet daily variation) field to calculate the disturbance field component.
- Coordinate transformation to a dipole system (i.e. one of the horizontal axes points in the geomagnetic dipole pole direction).
- Calculation of the longitudinally symmetric component (i.e. six-station average) and the asymmetric component (i.e. disturbance field minus the symmetric component).

Table 1. Stations used for the derivation of the ASY and SYM indices and related parameters at each station

Station name	ABB Code	G.G. Lat.	G.G. Long.	G.M. Lat.	G.M. Long.	Invariant Lat.	Rotation angle
San Juan	SJG	18.4	293.9	29.1	5.2	32.5	−8.9
Fredericksburg	FRD	38.2	282.6	49.1	352.2	50.4	0.4
Boulder	BOU	40.1	254.8	48.7	319.0	49.1	2.5
Tucson	TUC	32.3	249.2	40.4	314.6	39.7	2.7
Honolulu	HON	21.3	202.0	21.5	268.6	20.2	0.5
Memambetsu	MMB	43.9	144.2	34.6	210.2	34.9	−16.1
Martin de Vivies	AMS	−37.8	77.6	−46.9	142.8	48.6	−32.4
Hermanus	HER	−34.4	19.2	−33.7	82.7	43.6	−10.1
Chambon-la-Foret	CLF	48.0	2.3	50.1	85.7	45.7	−0.6

Distribution of geomagnetic observatories

Fig. 1. Distribution of the geomagnetic stations used for the derivation of the ASY and SYM indices

– Derivation of the asymmetric indices (i.e. the range between the maximum and the minimum asymmetric fields).
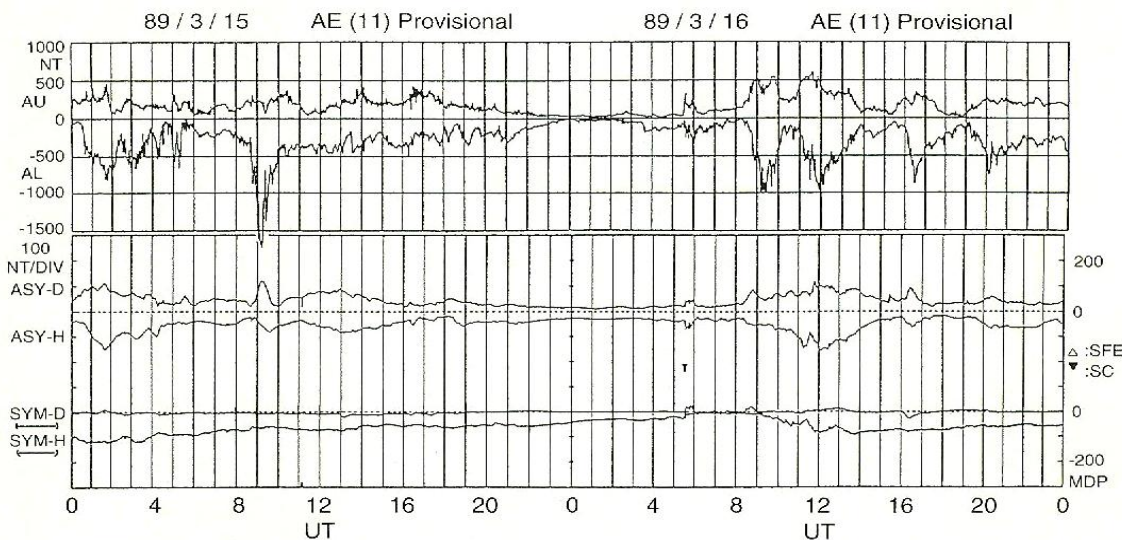
A more detailed description of the derivation and the characteristics of the indices are included in Iyemori (1990) and in Iyemori *et al.* (1992).

Figure 2 shows an example of the ASY and SYM indices for a storm period which started on 16 March 1989. The upper panel shows the provisional AU and AL indices, and the lower panel shows, from top to bottom, the ASY-D, ASY-H (positive downward), SYM-D (thin line) and SYM-H (thick line). A storm sudden commencement (SSC) is indicated by a solid triangle.

3 Some examples

Russell *et al.* (1974), Clauer and McPherron (1980) and Clauer *et al.* (1983) showed a closer relation of the Dst index or the asymmetric geomagnetic disturbances with the southward IMF than those with the AE indices. To check the role of the southward IMF, the

Fig. 2. The AU and AL indices (*upper panel*) and the ASY and SYM indices (*lower panel*) for a storm period. The SYM-H index (i.e. *thick line in the bottom panel*) is essentially the same as the Dst index

SEP 22 1987 (DAY 265)
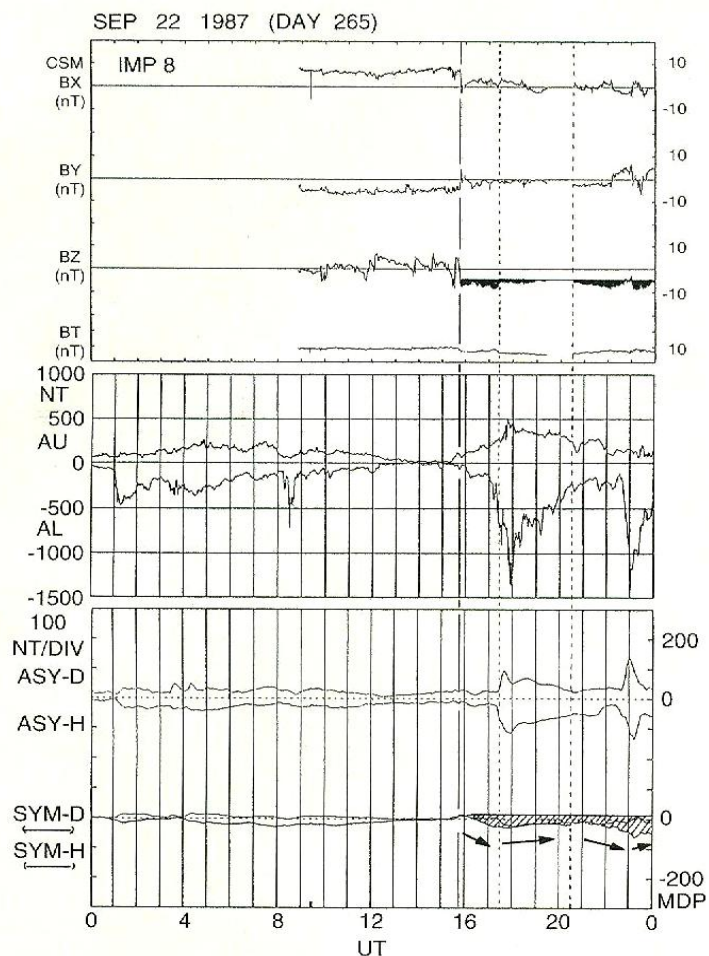
NOV 27 1990 (DAY 331)

Fig. 3. An example of the comparison of the AE, ASY and SYM indices with the IMF for a weak storm period. The *arrows in the bottom panel* emphasize the tendency of the Dst-field variation

Fig. 4. A comparison of the AE, ASY and SYM indices with the IMF for a storm period. The *arrows in the lower panel* indicate the onset time of substorms determined from the Pi2 pulsation onset on the ground

1-min-resolution IMF data constructed from the 15.36-s-resolution data from the IMP-8 magnetic field observation in the solar wind were used.

Figure 3 shows a case which would support the conclusion by Russell *et al.* (1974); the top panel shows the IMF variation, and the period where the southward component of the IMF exceeds 5 nT is blackened. According to Russell *et al.* (1974), the ring current develops when the southward component exceeds about 5 nT; the SYM-H trace in the bottom panel indicates a variation consistent with this conclusion. Although the substorm which started around 1725 UT is very large, the SYM-H (Dst field) does not develop, but decays. The Dst field develops during the strong southward IMF.

Figure 4 gives an example where the SYM-H starts to develop just after the southward turning of the IMF. The arrows in this figure indicate the substorm onset time defined by the mid-latitude Pi2 micropulsations detected in rapid-run magnetograms observed at Memambetsu, Japan and at Wingst, Germany. Although some substorm activities are seen before 1400 UT on 27 November, the decrease of the Dst component starts around 1400 UT when the IMF shows clear southward turning. At around 1600 UT and 1830 UT, where clear Pi2 onsets and an increase in asymmetric distur-
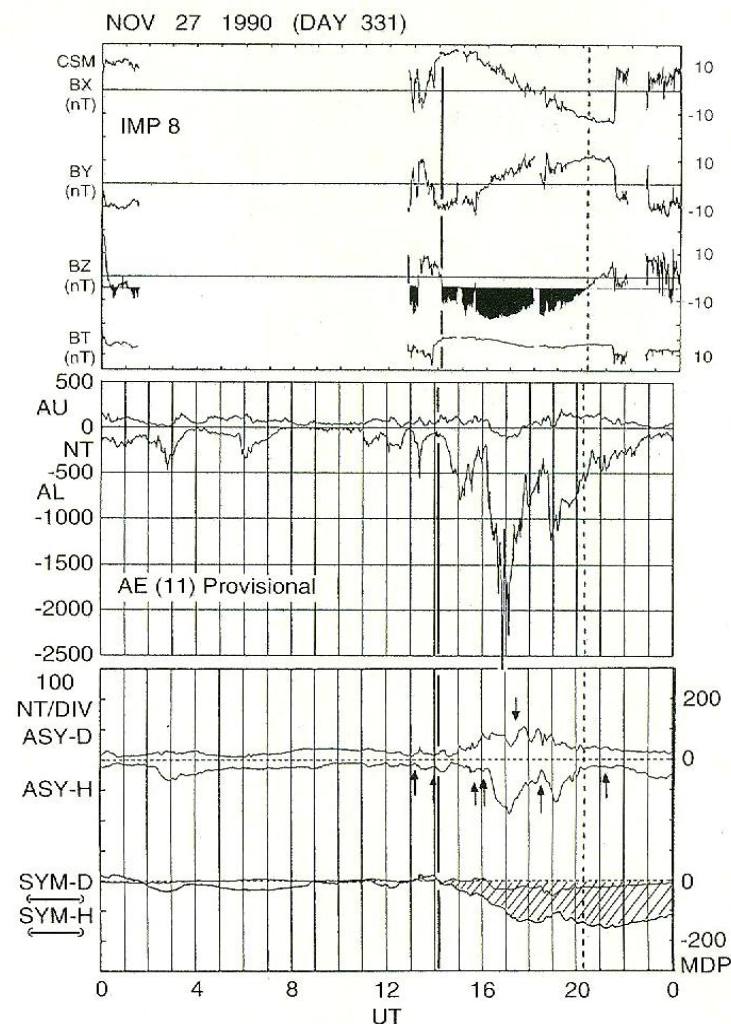
bances are observed, the Dst component shows a slight recovery.

Figure 5 also shows a comparison between the IMF and the ASY/SYM indices. When the IMF has a strong southward component during the period from 1700 UT 25 April to 0100 UT 26 April, the SYM-H is seen to develop. However, although clear substorm onsets, as in the case of 1900–2200 UT on 26 April are noticed, the Dst would not have developed in the absence of a strong southward component of the IMF.

These examples suggest a closer relation of the development of Dst field to the IMF southward component than to the substorm activity. In the following sections, this tendency is statistically confirmed.

4 Method of statistical analysis

4.1 Substorms defined by a mid-latitude positive-bay onset

A substorm onset is defined by a rapid increase of the ASY-D or ASY-H index having the characteristic shape of
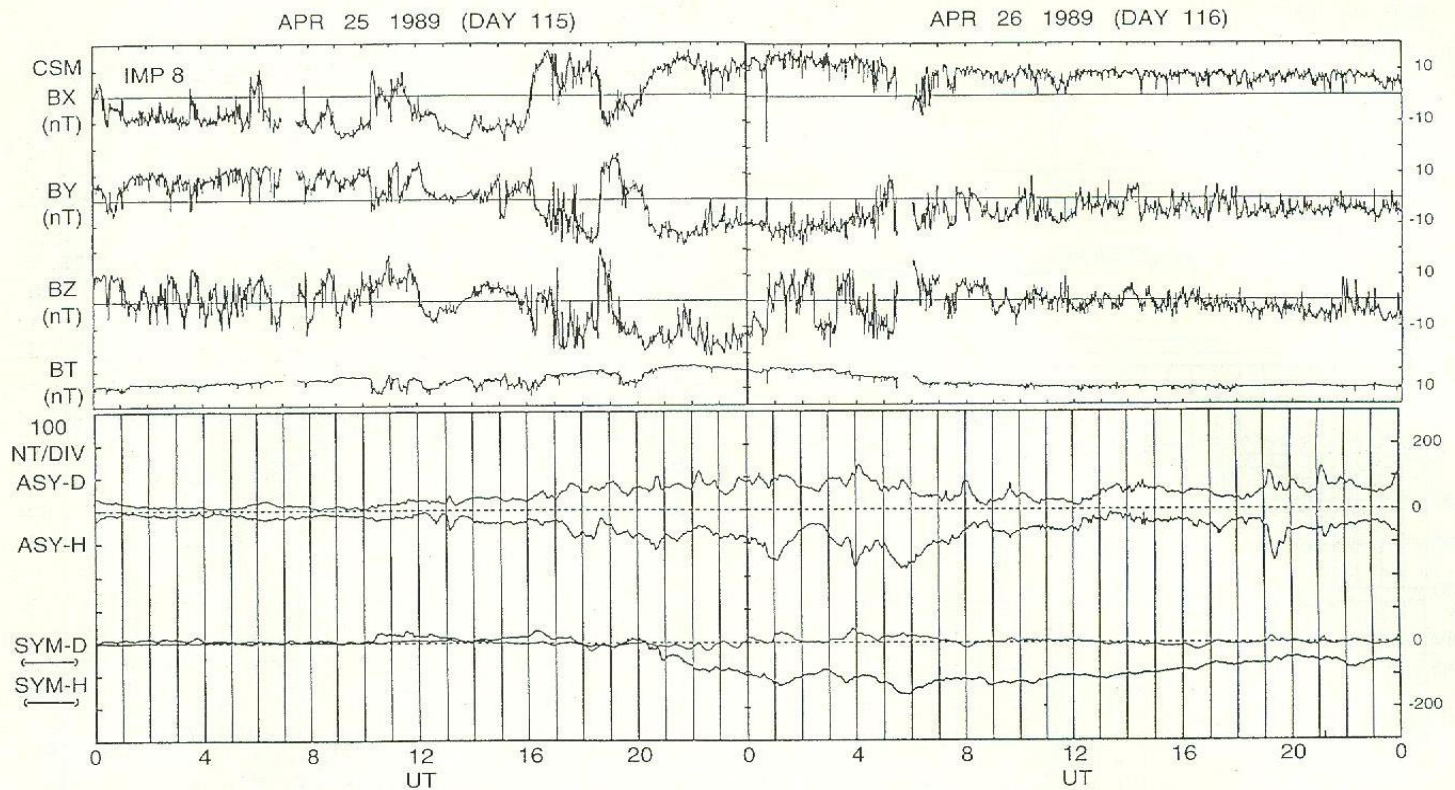
Fig. 5. Another example of the comparison of the ASY-SYM indices with the IMF

mid-latitude positive bay (e.g. Rostoker *et al.*, 1980). A large positive-bay onset is seen in Fig. 2 at 0853 UT on 15 March, and at around 1600 UT on 16 March. Magnetospheric compression by interplanetary shock waves or discontinuities can be distinguished from mid-latitude positive bay by looking at the SYM-H index, because the shape of the former is generally much steeper for shock events than that for positive bays (as is seen in an SSC event at 0530 UT on 16 March). The event (i.e. positive-bay) selection was made using two methods: by eye inspection and by a computer pattern-matching technique. In the eye inspection, the intervals were limited to the storm periods where the minimum of the SYM-H (i.e. the Dst) index was less than −100 nT, and the criteria for event selection using this technique are:
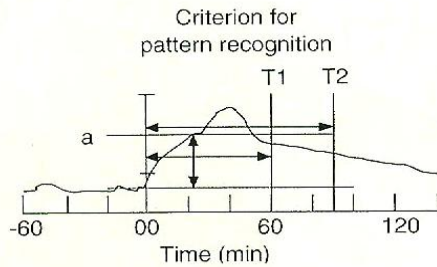
– An amplitude increase of more than 20 nT in at least one of the ASY-D and ASY-H indices within 30 min.
– A shape which is round topped and a timescale span of about 30–60 min: the general characteristics of mid-latitude positive bays.

The start of the increase is defined as the onset time, T = 0. The second criterion is in order not only to select typical mid-latitude positive bays but also to exclude sudden commencements or sudden impulses which are caused by the sudden change in solar-wind dynamic pressure due to various types of discontinuities. The positive bays with amplitude greater than 20 nT correspond to, in general, rather large substorms measured by the AE indices. From 28 storm periods which occurred during 1989–1990, 186 substorm events were selected. The storm periods and number of substorms selected are given in Table 2. These events are divided into two groups; one is

Table 2. List of geomagnetic storms in 1989 and 1990 and number of substorm onsets in each storm period that satisfied the criterion for eye inspection (see text)

	Storm period	No. of events	
		Main	Recovery
1	Jan. 11–12, 1989	1	2
2	Jan. 15–16, 1989	5	4
3	Jan. 20–22, 1989	2	6
4	Mar. 13–15, 1989	3	3
5	Apr. 25–26, 1989	5	4
6	May 23–25, 1989	2	1
7	Jun. 10, 1989	2	2
8	Aug. 11, 1989	0	2
9	Aug. 14–18, 1989	5	5
10	Aug. 28–30, 1989	2	4
11	Sep. 18–19, 1989	6	2
12	Sep. 26, 1989	4	1
13	Oct. 20–23, 1989	7	8
14	Nov. 17–18, 1989	1	3
15	Feb. 16, 1990	4	4
16	Mar. 12–15, 1990	3	4
17	Mar. 20–21, 1990	2	3
18	Mar. 30, 1990	2	0
19	Apr. 10–18, 1990	6	17
20	Apr. 23–25, 1990	3	2
21	May 22, 1990	3	0
22	May 27, 1990	1	1
23	Jun. 12–14, 1990	3	0
24	Jul. 28–29, 1990	4	1
25	Aug. 22–24, 1990	4	5
26	Aug. 26, 1990	3	0
27	Oct. 10–12, 1990	4	11
28	Nov. 27–28, 1990	2	2
Total		89	97

Fig. 6. A schematic drawing of the criterion of automatic event (i.e. mild-latitude positive bay) selection

for the events occuring in the storm main phase and the other occuring during the recovery phase. The main and the recovery phases are defined as the periods before and after the times when the Dst (SYM-H) reached its minimum value.

For the other event-selection technique, pattern matching, the criteria adopted are as follows (see Fig. 6):

– An increase in ASY-D (or ASY-H) of more than 30 nT within 60 min.
– A decrease to two-thirds of the peak value within 90 min.

To avoid the effect of short-timescale fluctuations, 5-min averages of the ASY indices are used. In this selection, we did not limit ourselves to the storm times used in the case of the eye selection, but took the entire period 1989–1990.

4.2 Substorms defined by a sharp decrease in the AL index

A sharp decrease in the AL index, which is supposed to indicate the rapid development of the westward electrojet in the auroral zone, is used to define a substorm onset. The 1-min-resolution AL index for 1985 is used. The criteria are: a decrease in the AL index of more than 300 nT (resp. 600 nT) within 10 min; an interval between successive onsets of more than 30 min. A total of 634 onsets (resp. 67) are selected for the criterion of a decrease of more than 300 nT (resp. 600 nT). The start time of the sharp decrease is taken as the onset time.

4.3 Substorms defined by a clear Pi2 onset

A clear Pi2 onset is used to define a substorm onset (e.g. Rostoker *et al.*, 1980). The list of the Pi2 pulsations obtained at Memambetsu for 1984 and 1985 published by the Kakioka Magnetic Observatory (1985, 1986) are used. The Pi2 pulsations are classified as A, B and C by the observatory and we used the clear Pi2 onsets which are classified as A or B in their list. We did not adopt the second or the third onset of the multiple-onset substorms if it was observed within 30 min of the first.

5 Results

5.1 Substorms defined by a mid-latitude positive-bay onset

In each substorm event, the SYM-H index increases in some cases and decreases in others, as seen in Figs. 2–5. For example, a very large substorm onset is observed in the AE indices at 0853 UT on 15 March as seen in Fig. 2. However, the SYM-H index does not show any appreciable decrease after the onset; a similar tendency is observed at around 1600 and 2000 UT on 16 March. On the other hand, the SYM-H starts decreasing at around 0900 UT on the same day. If the substorms are the causes of the ring-current development, and if the SYM-H index indicates the ring-current intensity, the SYM-H should develop (i.e. its negative value increases) after each substorm onset. To check this expectation statistically, each of the ASY-D, ASY-H, and SYM-H indices are superimposed for the substorm events selected by the relevant criterion and the average pattern of variation around the onset is obtained. The time T = 0 in Figs. 7 and 8 indicates the substorm onset. The error bars in each of the figures are the standard deviation divided by the square root of the number of events superimposed (standard error).

Figure 7 shows the cases where the events were selected by eye inspection. It is clear that the Dst (SYM-H) field does not show any development after the onset. The slope of the SYM-H indicates a sudden change to positive direction rather than the expected negative. This tendency is more clearly seen in the case for storm recovery phase (lower panel in Fig. 7). The shape is stepwise rather than that of a typical positive bay with timescale of about 1 h.

Figure 8a, b shows the results of superposed epoch analysis for the substorm events selected by pattern-matching procedure. In this case, the events are divided into two groups. In one group, the correlation coefficient between the ASY-H and SYM-H for 30 min just after the epoch, T = 0, is positive, i.e. the SYM-H increases. In another case, the correlation is negative, indicating that the SYM-H decreases (i.e. the Dst field develops). Figure 8a shows the results for the events selected by the ASY-D index and Fig. 8b the cases selected by the ASY-H. Even for the 'negative-correlation' events, the slope of the SYM-H becomes more gentle after the onset.

None of the cases shown in Figs. 7 and 8 indicate the development of the SYM-H (Dst) index, i.e. a more negative tendency in the slope, after the onset time. Contrary to expectations, it decays, or the slope becomes more gentle, after substorm onset. The SYM-H component does not show any tendency toward development for at least 8 h after substorm onset, indicating that the aftereffect of a substorm on the Dst component is negligible. This result suggests that a substorm onset does not play any significant role in the ring-current development.

5.2 Substorms defined by a sharp decrease in the AL index

Figure 9 shows the results of a superposed epoch analysis for the substorms defined by a sharp decrease in the AL
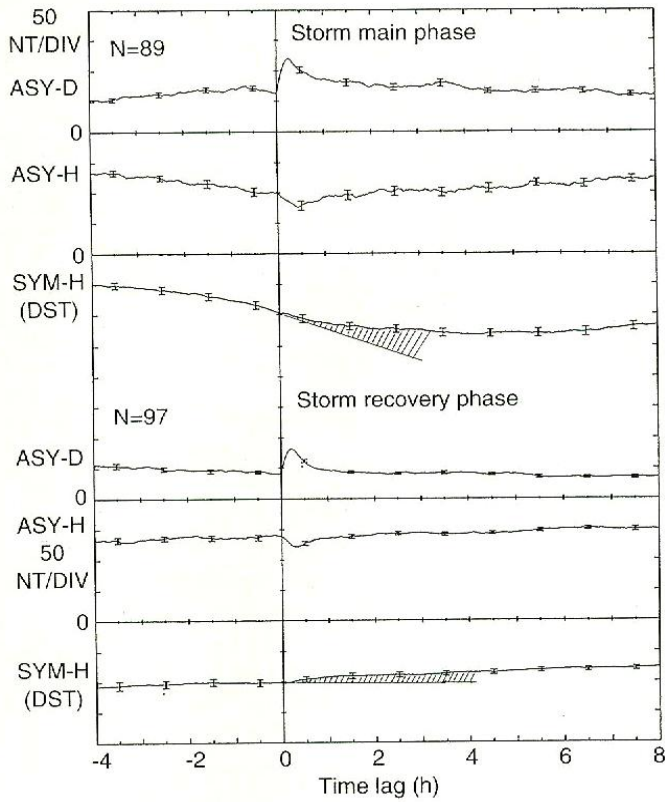
Fig. 7. Averaged behaviour of the ASY and SYM indices at substorm onset. The events selected by eye inspection are divided into two groups, one group is in the storm main phase and another in the recovery phase; they are superimposed and averaged separately
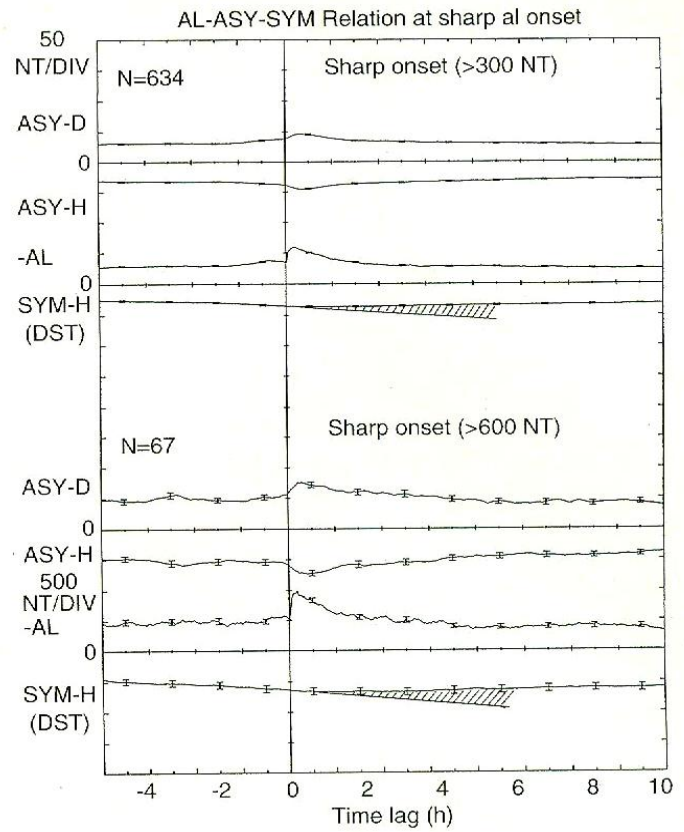
Fig. 9. Results for the substorm events defined by a sharp decrease in the AL index for the period in 1985. The scale of the AL index is ten times greater than that of the ASY and SYM indices, and negative upward

index. The traces in the upper half of the figure indicate the ASY-D, ASY-H, −AL (i.e. negative upward) and SYM-H (Dst) indices around the onset time for the events where the AL index decreased by more than 300 nT within 10 min. The scale for the AL index is ten times greater than those of other indices; that is, one tick mark

corresponds to 500 nT. The traces in the lower half of the figure are for the cases where the AL index decreased by more than 600 nT within 10 min. In both cases, the Dst field tends to recover after the onset time, which is consistent with the result for the positive bay substorms.
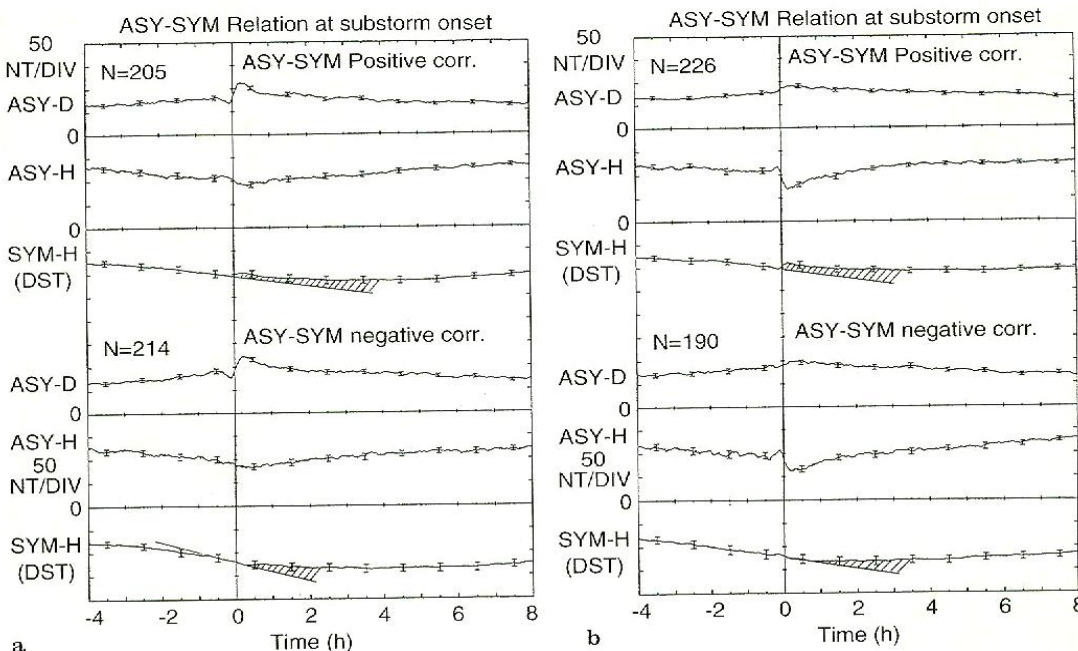
Fig. 8. Results of a superposed epoch analysis for the events selected automatically by a criterion shown in Fig. 3. The events were selected using the ASY-D index (*left panel*) and the ASY-H (*right panel*)

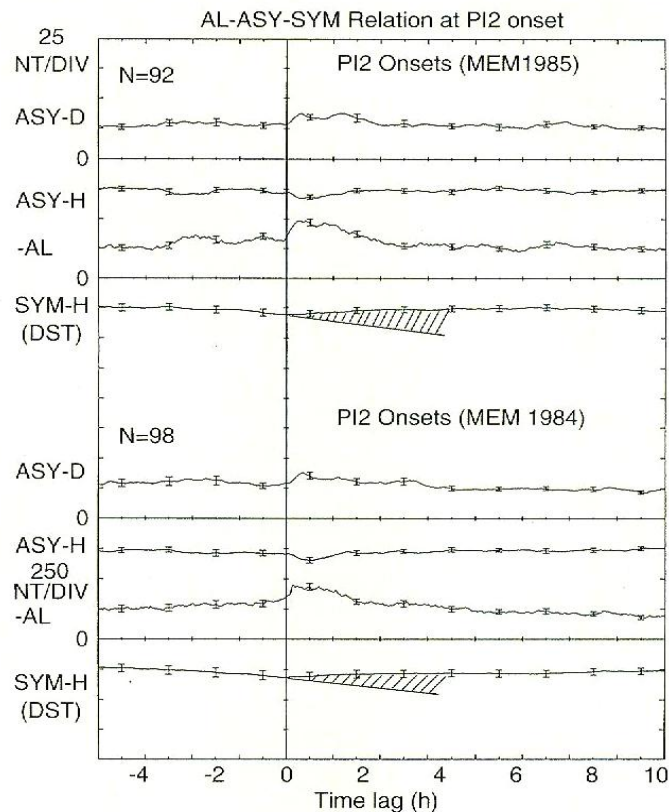## 5.3 Substorms defined by a clear Pi2 onset

Figure 10 shows the results for the substorms defined by a clear Pi2 onset. The traces show the same indices as those in Fig. 7, though the scale is expanded to show the variation more clearly. The upper half of the figure shows the results for the events in 1984 and the lower half for those in 1985. The Dst field in this case also shows the tendency toward recovery after substorm onset.

5.4 IMF variation

Figure 11a, b shows the results of the superposed epoch analysis for the substorm events during the intervals of the availability of IMF data. The substorm onsets are those of the positive-bay onset that were selected by eye inspection, and thus they are the subset of the events presented in Fig. 7. The results for the ASY and SYM indices are essentially the same as before (presented in Figs. 7 and 8). The results for storm main phase indicate that the Dst field starts to develop when the IMF southward component becomes less than -5 nT, i.e. more than one hour before the substorm onset time, as has been suggested as a criterion for ring-current development (Russell et al., 1974). The results for the storm recovery phase indicate that the recovery of the SYM-H (Dst) is synchronized with the substorm onset. Thus, the development of the Dst field appears to be correlated with the southward IMF, its decay with the substorm onset.
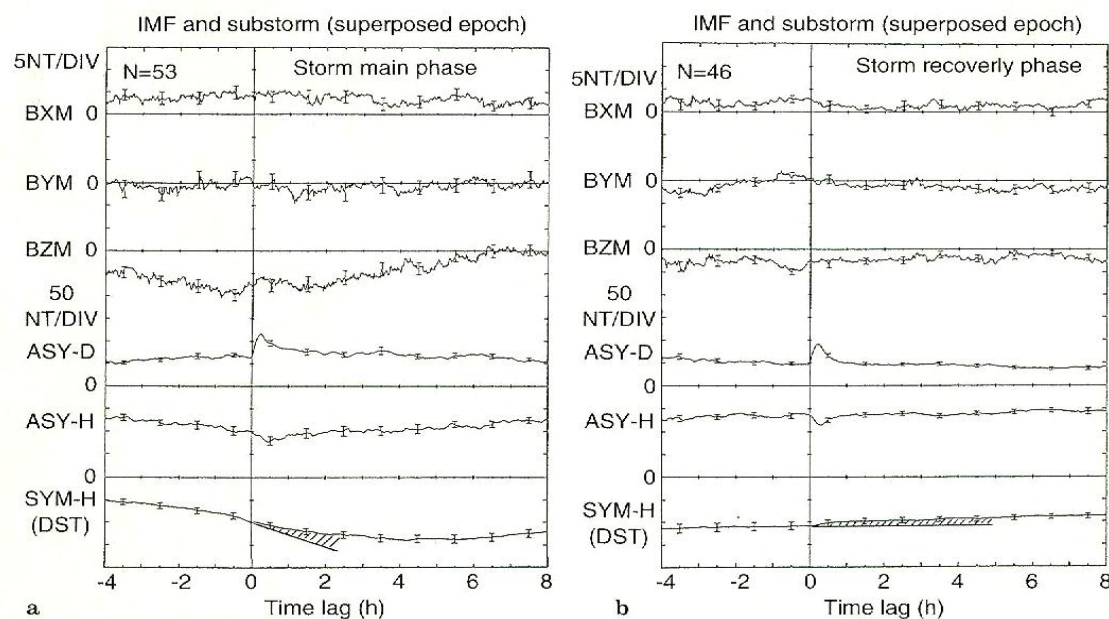
6 Discussion

The recovery of the SYM-H index just after substorm onset as indicated in Figs. 7–11 suggests that the particle injection observed at synchronous orbit after substorm onset (e.g. Kamide and McIlwein, 1974) is not the main cause of the ring-current development. In order to see the

Fig. 10. Results for the events defined by a clear Pi2 onset taken from the list obtained at Memambetsu magnetic observatory
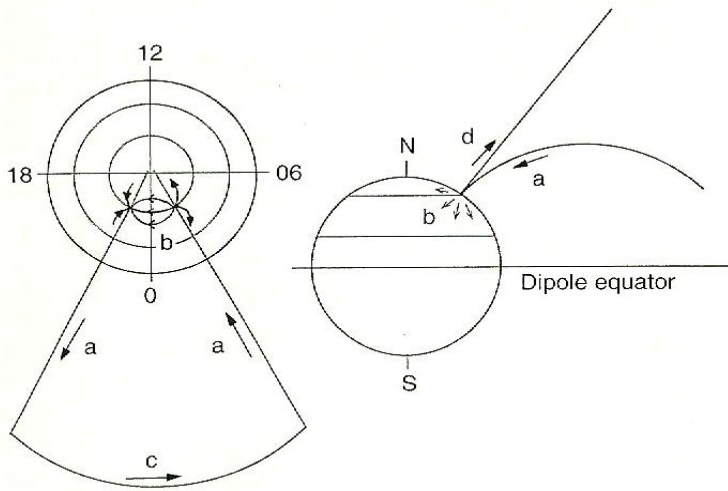
current system responsible for the recovery of the SYM-H after substorm onset, the magnetic effects on the ground of a simple current circuit, the 'substorm wedge current' (e.g. Nagai, 1982) are calculated.

Figure 12 is a schematic drawing of the system and Fig. 13 shows the magnetic fields generated by the current circuit on the ground. The magnetic fields generated by the current system are estimated integrating Biot-Savart's law, as has been done by Kamide and Fukushima (1971)

Fig. 11. Results of a superposed epoch analysis for the substorm events to show the average IMF behavior before and after the substorm onset
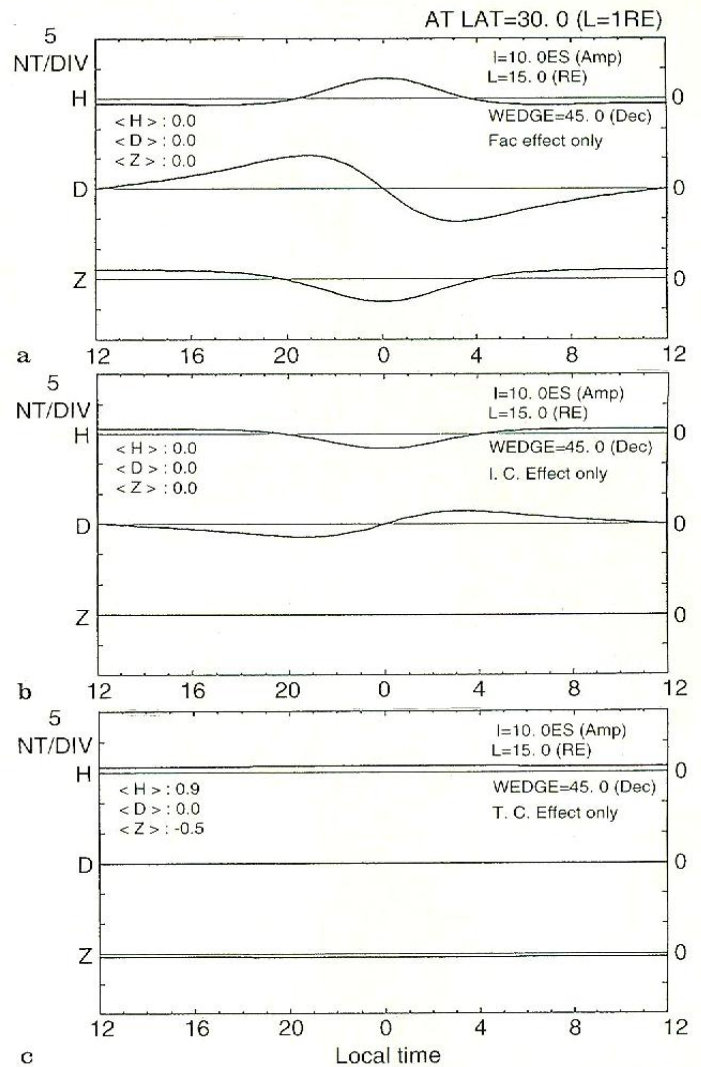
Fig. 12. A schematic drawing of the substorm wedge current system. The ground geomagnetic fields generated by each part of this circuit are calculated separately by Biot-Savart's law. The ionospheric Pedersen current is replaced by the straight vertical current applying Fukushima's theorem

for the so-called 'partial ring-current system' with a slightly different assumption on the ionospheric current part. The local time dependence of the components at 30° latitude is shown. The circuit is divided into three parts: a field-aligned current along the main dipole field, an ionospheric Pedersen current, and a tail current. The ionospheric Pedersen conductivity is assumed to be uniform. The 'disrupted' tail current was replaced by the partial dusk-to-dawn current as shown in Fig. 12. The Hall current is not calculated even under the simple uniform-conductivity assumption for a reason given later in this section. The effect of the Pedersen current is calculated by replacing it with a straight vertical current applying Fukushima's theorem (Fukushima, 1971, 1976). The ionospheric current might be too simple, and a more realistic distribution of the ionospheric conductance should be used for a more accurate representation.

The SYM-H (Dst) index is essentially an average of the disturbance in the horizontal component observed at mid-latitude stations distributed in longitude. Figure 13 shows the local time dependence of the magnetic effects from each part of the circuit. The local time variation of the sum of these three effects, that is, a clear positive peak in H component around local midnight and the small negative H component on the dayside, are consistent with that of the bay disturbances obtained by Silsbee and Vestine (1942). In this figure the magnetic effects from the northern-hemispheric part of the current system and those from the equatorial current are shown. The magnetic effects from the southern part of the field-aligned currents are in the opposite direction for the D component with less magnitude, and in the same direction for the H component with almost the same magnitude. Therefore the effect in the D component is weakened and that in the H component strengthened if we take into account the effects from southern-hemispheric currents. At 30° latitude in the northern hemisphere, the magnitude for the D com-

Fig. 13. The magnetic-field variation in local time at 30° in the northern hemisphere estimated for a substorm wedge current system. The effects from each current part shown in Fig. 9 are calculated by Biot-Savart's law and shown in a local H, D and Z coordinate system. Panel (a) indicates the effect from field-aligned currents along geo-dipole, (b) that from ionospheric Pedersen currents and (c) that from tail currents. The average in local time is exactly zero for traces in (a) and (b), but finite for (c). The current intensity, the geocentric distance of the tail-current part, and the angle of the wedge currents (i.e. the longitudinal extent) are 10^6 A, 15 Re and 45°, respectively, in this example. The average in local time for each component is shown in the upper left corner of each panel

ponent is about half of that shown in Fig. 13, and is almost doubled for the H component.

The average effect of the field-aligned-current in magnetic local time (i.e. in longitude) is zero for the above current system. This is the same even if the effects from the southern-hemispheric current system are added. The effect from the ionospheric Pedersen current also disappears by the averaging process. These results have been predicted by Siscoe and Crooker (1974) considering the symmetry of the current system. The Hall-current effect also becomes negligible if uniform conductance is assumed and if the symmetry of the current system is taken into account. Only the tail-current effect is not cancelled out and remains. This simple calculation suggests that the decay

(increase) of the SYM-H just after substorm onset is caused by the decrease (weakening) of the dawn-to-dusk tail current. This is consistent with the weakening of the field strength in the magnetotail lobe after substorm onset (Caan et al., 1978). The difference between the shape of variation after T = 0, i.e. the stepwise recovery of the SYM-H index for the case shown in Fig. 7 (lower panel), and that of the positive bay also supports the idea, because the effect of the current disruption (i.e. weakening of the tail current) remains even if the wedge current system disappears.
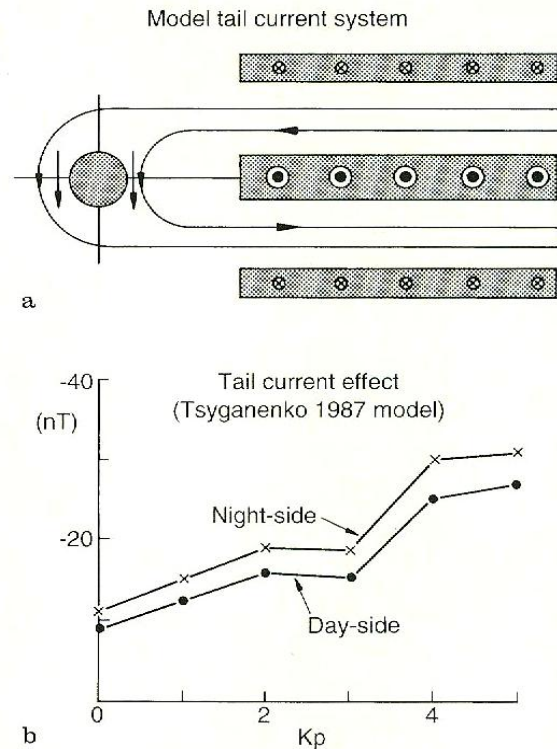
The magnetic effect of magnetospheric tail current on the earth is estimated using the long version of the Tsyganenko 1987 model (Tsyganenko, 1987) by calculating the contribution from its tail-current part. Figure 14a shows a schematic drawing of the tail-current system used in the model and its magnetic effect at the earth viewed from dusk side. Figure 14b shows the Kp-index dependence of the tail-current effect on both the dayside and the nightside of the earth's surface. The difference between disturbed (Kp = 4 or 5) and quiet conditions (Kp = 1 or 2) is about 10–15 nT, which is close to the magnitude of the recovery after substorm onset observed in the SYM-H (Dst) field.

These results of data analysis and simple model calculations suggest that the recovery of the Dst field after a substorm onset is caused by the decay of the tail current. That is, the contribution to the Dst field of particle injection to the inner magnetosphere associated with a substorm onset is negligible, and the contribution of tail-current decay after the onset more significant for the earth than the substorm injection effect.

The decay of the Dst field is understandable because it indicates not only the ring-current particle energy (Dessler and Parker, 1959; Sckopke, 1966), but also the particle and field energies of various current systems in the magnetosphere, including the tail current (Siscoe, 1970).

Sometimes during the great geomagnetic storms (e.g. when the occasions of the low-latitude red aurora are observed) the Dst rapidly decays after the substorm onset. For example, at around 1130 UT on 21 October 1989, 0330 UT on 25 March 1991, or 0400 UT on 9 November 1991, the Dst field does not develop but decays after large substorm onset. Such phenomena may be understood by adopting the idea that the substorm is a process which dissipates the energy stored in the magnetosphere, and that the Dst field indicates not only the ring-current particle energy but also the field and particle energy of various current systems in the magnetosphere, as shown by Siscoe (1970) for an ideal case, viz. steady and closed system.

The better correlation of the Dst development with a strong southward IMF, rather than with substorm activity (e.g. Figs. 3–5 in this paper; Russell et al., 1974), suggests the importance of magnetospheric convection for ring-current development (e.g. Takahashi et al., 1991, and references therein). The results shown in this paper support the idea that the geomagnetic storms and substorms are independent processes, and that the ring-current development is not the result of the frequent occurrence of substorms but the result of enhanced convection caused

Fig. 14. *Upper panel*: a schematic drawing of the tail-current system in the Tyganenko 1987 model (long version). *Lower panel*: the Kp-index dependence on its magnetic effects on dayside equator (*solid circles*) and those on nightside equator (*cross marks*)

by the large southward IMF. A substorm is the process of energy dissipation in the magnetosphere, and its contribution to the storm-time ring-current formation seems to be negligible. In the future this point should be quantitatively shown by energetic-particle measurements, because from the geomagnetic measurements on the ground only, we cannot distinguish the fields of the ring current which flow in the inner magnetosphere from those of the tail-current fields.

In the proof of the theorem by Siscoe (1970), a closed system in a steady state was assumed. However, the magnetosphere is believed to be an open system magnetically connected with the interplanetary space and is not in a steady state. Therefore we need to estimate the approximate distance and timescale where the theorem is applied. From the results of the superposed epoch analysis shown in Figs. 7–10 and by the estimation of simple tail-current effects, the theorem appears to be valid for the magnetosphere including near-earth tail current. The quantitative validity and the limitation on the application of the theorem should in future be examined by a computer-simulation technique.

References

Akasofu, S.-I., and S.Chapman, *Solar-Terrestrial Physics*, Oxf. Univ. Press, 1972.

Caan, M. N., R. L. McPherron, and C. T. Russell, The statistical magnetic signature of magnetospheric substorms, *Planet. Space Sci.*, **26**, 269–279, 1978.

Clauer, C. R., and R. L. McPherron, The relative importance of the interplanetary electric field and magnetospheric substorms on the partial ring current development, *J. Geophys. Res.*, **85**, 6747–6759, 1980.

Clauer, C. R., McPherron, R. L., and C. Searls, Solar wind control of the low-latitude asymmetric magnetic disturbance field, *J. Geophys. Res.*, **88**, 2123–2130, 1983.

Crooker, N. C., and G. L. Siscoe, A study of the geomagnetic disturbance field asymmetry, *Radio Sci.*, **6**, 495–501, 1971.

Dessler, A. J., and E. N. Parker, Hydromagnetic theory of geomagnetic storms, *J. Geophys. Res.*, **64**, 2239–2252, 1959.

Fukushima, N., Electric current systems for polar substorms and their magnetic effect below and above the ionosphere, *Radio Sci.*, **6**, 269–275, 1971.

Fukushima, N., Generalized theorem for no ground magnetic effect of vertical currents connected with Pedersen currents in the uniform-conductivity ionosphere, *Rep. Ionos. Space Res. Japan*, **30**, 35–40, 1976.

Fukushima, N., and Y. Kamide, Partial ring current models for worldwide geomagnetic disturbances, *Rev. Geophys. Space Phys.*, **11**, 795–853, 1973.

Gonzalez, W. D., J. A. Joselyn, Y. Kamide, H. W. Kroehl, G. Rostoker, B. T. Tsurutani, and V. M. Vasyliunas, What is a geomagnetic storm? *J. Geophys. Res.*, **99**, 5771–5792, 1994.

Iyemori, T., Storm-time magnetospheric currents inferred from mid-latitude geomagnetic field variations, *J. Geomag. Geoelectr.*, **42**, 1249–1265, 1990.

Iyemori, T., T. Araki, T. Kamei, and M. Takeda, *Mid-latitude geomagnetic indices ASY and SYM (provisional) No. 1 1989*, Data Analysis Center for Geomag. and Space Magnetism, Kyoto Univ., Kyoto, 1992.

Kakioka Magnetic Observatory, *Report of the geomagnetic and geoelectric observations 1984 (rapid variations)*, **No. 25**, p. 8–9, Kakioka, Japan, 1985.

Kakioka Magnetic Observatory, *Report of the geomagnetic and geoelectric observations 1985 (rapid variations)*, **No. 26**, p. 8–9, Kakioka, Japan, 1986.

Kamide, Y., Is substorm occurrence a necessary condition for a magnetic storm? *J. Geomag. Geoelectr.*, **44**, 109–117, 1992.

Kamide, Y., and N. Fukushima, Analysis of magnetic storms with DR-indices for equatorial ring current field, *Rep. Ionos. Space Res. Japan*, **25**, 125–162, 1971.

Kamide, Y., and C. E. McIlwain, Onset time of magnetospheric substorms determined from ground and synchronous satellite records, *J. Geophys. Res.*, **79**, 4787–4790, 1974.

Kawasaki, K., and S.-I. Akasofu, Low-latitude DS component of geomagnetic storm field, *J. Geophys. Res.*, **76**, 2396–2405, 1971.

Nagai, T., Observed magnetic substorm signatures at synchronous altitude, *J. Geophys. Res.*, **87**, 4405–4417, 1982.

Rostoker, G., S.-I. Akasofu, J. Foster, R. A. Greenwald, Y. Kamide, K. Kawasaki, A. T. Y. Lui, R. L. McPherron, and C. T. Russell, Magnetospheric substorms – Definition and signatures, *J. Geophys. Res.*, **85**, 1663–1668, 1980.

Russell, C. T., R. L. McPherron, and R. K. Burton, On the cause of geomagnetic storms, *J. Geophys. Res.*, **79**, 1105–1109, 1974.

Sckopke, N., A general relation between the energy of trapped particles and the disturbance field near the Earth, *J. Geophys. Res.*, **71**, 3125–3130, 1966.

Silsbee, H. C., and E. H. Vestine, Geomagnetic bays, their frequency and current systems, *Terr. Magn. Atmos. Electr.*, **47**, 195–208, 1942.

Siscoe, G. L., The virial theorem applied to magnetospheric dynamics, *J. Geophys. Res.*, **75**, 5340–5350, 1970.

Siscoe, G. L., and N. U. Crooker, On the partial ring current contribution to Dst, *J. Geophys. Res.*, **79**, 1110–1112, 1974.

Sugiura, M., and D. J. Poros, *Hourly values of geomagnetic Dst for the years 1957 to 1970*, Goddard Space Flight Center Preprint X-645-71-278, 1971.

Takahashi, S., T. Iyemori, and M. Takeda, A simulation of the storm-time ring current, *Planet. Space Sci.*, **38**, 1133–1141, 1990.

Tsyganenko, N. A., Global quantitative models of the geomagnetic field in the cislunar magnetosphere for different disturbance levels, *Planet. Space Sci.*, **35**, 1347–1358, 1987.